Communication

A Monomeric Mn#Peroxo Complex Derived Directly from Dioxygen

Ryan L. Shook, William A. Gunderson, John Greaves,
Joseph W. Ziller, Michael P. Hendrich, and A. S. Borovik

J. Am. Chem. Soc., **2008**, 130 (28), 8888-8889 • DOI: 10.1021/ja802775e • Publication Date (Web): 21 June 2008

J|A|C|S
COMMUNICATIONS

Published on Web 06/21/2008

A Monomeric Mn^{III}−Peroxo Complex Derived Directly from Dioxygen

Ryan L. Shook,[†] William A. Gunderson,[‡] John Greaves,[†] Joseph W. Ziller,[†] Michael P. Hendrich,[‡] and A. S. Borovik*,[†]

Department of Chemistry, University of California—Irvine, 1102 Natural Sciences II, Irvine, California 92697-2025, and Department of Chemistry, Carnegie Mellon University, Pittsburgh, Pennsylvania 15213

Received April 15, 2008; E-mail: aborovik@uci.edu

The binding and activation of dioxygen is an essential process in synthetic and biological chemistry.[1] The activation processes are often proposed to involve formation of peroxometal complexes, as exemplified by bleomycin and the mono-oxygenases cytochromes P450.[2] It is generally agreed that the initial steps in the O_2 binding/activation process in these enzymes involve a superoxoiron(III) intermediate that converts to a hydroperoxoiron(III) species through addition of an electron and proton. In this report, we demonstrate that a similar O_2 to peroxo conversion is operable in a synthetic manganese system.

The observation of synthetic monomeric peroxometal complexes is frequently difficult because of their inherent reactivity. This is especially true for peroxomanganese complexes, where the $Mn^{IV}_2(\mu$-1,2-peroxo) complex of Wieghardt is the only O_2-derived system that has been structurally characterized.[3,4] Others have found that treating Mn^{II} or Mn^{III} complexes with superoxides[5] or peroxides[6] produce systems with monomeric peroxomanganese centers—this approach has yielded a handful of complexes at low temperatures that were stable enough to be characterized. We have been investigating the interactions of dioxygen with manganese complexes containing intramolecular hydrogen bonding (H-bond) networks.[7] Our systems utilize urea-based tripodal ligands that provide H-bond donors to coordinated O-atom species. The Mn^{II} complexes of these ligands bind and activate dioxygen producing monomeric oxomanganese complexes.[7,8] We have developed a hybrid ligand (H_5bupa) that combines two urea arms with one carboxyamidopyridyl moiety[9]—the Mn^{II} complex of this ligand binds O_2 to produce a detectable peroxomanganese(III) species.

Preparation of the precursor **1** is outlined in Figure 1.[10] Treating H_5bupa with 3 equiv of KH in dimethylacetamide (DMA) followed by 1 equiv of $Mn(OAc)_2$ afforded K[**1**] and 2 equiv of KOAc.

The molecular structure of **1** determined by X-ray diffraction shows a five-coordinate Mn^{II} complex, having a distorted trigonal bipyramidal geometry.[10] The trigonal plane is defined by the deprotonated urea and pyridyl nitrogen atoms of $[H_2bupa]^{3-}$; the apical N1 atom and carbonyl oxygen O1 from the deprotonated carboxamide occupy the axial positions. The remaining portions of the urea groups form the scaffolding of a cavity, in which NH groups are positioned inward toward atom O1. However, the N6(N7)···O1 distances are greater than 3.2 Å, distances that are too long for intramolecular H-bonds.

A new green species (**2**) is formed in approximately 50% yield[11] when $[Mn^{II}H_2bupa]^-$ reacts with O_2 at room temperature. In DMA, the reaction is relatively slow (~30 min), yet the formation of **2** can be completed in approximately 10 min when 0.5 equiv of diphenylhydrazine (DPH) is added to the reaction mixture (Figure 1). The yield of **2** also increases to nearly 80% when using DPH,

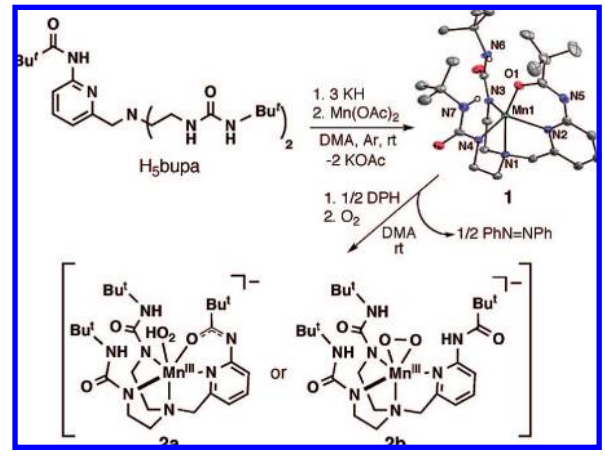

Figure 1. Preparative routes for **1** and **2**, showing two possible tautomers for **2**. The thermal ellipsoid plot of $[Mn^{II}H_2bupa]^-$ is drawn at the 50% probability level, and non-urea hydrogen atoms are omitted for clarity. Selected distances (Å): Mn1−N1, 2.275(3); Mn1−N2, 2.214(3); Mn1−N3, 2.100(3); Mn1−N4, 2.125(3); Mn1−O1, 2.070(2).

which is converted to azobenzene (>95% yield). Monitoring the reactions with optical spectroscopy shows that **2** has a visible absorbance band at $\lambda_{max} \approx 660$ nm and a shoulder at 490 nm (Figure S1).[12] Similar spectra have been reported for Mn^{III} complexes containing a coordinated peroxo ligand.[5d,6b]

The oxygenation of **1** was followed by electron paramagnetic resonance (EPR) spectroscopy (Figure S2). Perpendicular-mode X-band EPR spectra of $[Mn^{II}H_2bupa]^-$ reveal the complex as a nearly axial $S = 5/2$ spin system with a large zero-field splitting constant of $D \sim 0.3$ cm^{-1}. After exposure to O_2, the $S = 5/2$ signal decreases as a new parallel-mode EPR signal associated with **2** appears at a g value of 8.2 (Figure 2A). A quantitative simulation of the signal (Figure 2B) indicates an $S = 2$ ground state with a six-line ($I = 5/2$) hyperfine splitting of $a = 57$ G. Variable temperature studies determined that the signal is from the ground doublet with $D = -2.0(5)$ cm^{-1}. The spin state, zero-field splitting, and hyperfine constant are in agreement with other known monomeric Mn^{III} species.[5d,13] Moreover, the negative sign for the axial zero-field splitting constant is consistent with tetragonally elongated octahedral coordination geometry. The simulations also indicate that **2** accounts for 80(10)% of the Mn in the sample. In perpendicular-mode, this sample also showed the signal of the initial Mn(II) complex (6%) and a mixed valent species at $g = 2$ (4%). The parallel-mode signal vanishes after prolonged incubation (6 h) at room temperature—the identity of the resultant species are under investigation.

Isotopic labeling studies support the presence of a peroxo ligand coordinated to the Mn^{III} center in **2**. Solution FTIR spectra recorded at room temperature contained a peak at 885 cm^{-1} for **2** prepared

[†] University of California—Irvine.
[‡] Carnegie Mellon University.

10.1021/ja802775e CCC: $40.75

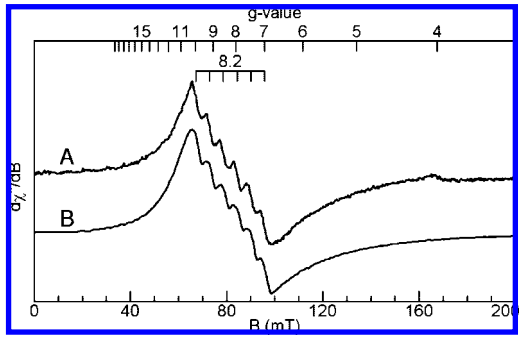

Figure 2. Parallel-mode EPR spectrum (A) and simulation (B) of **2** (10 mM in DMF) recorded at 11 K. Microwave frequency and power, 9.379 GHz, 0.2 mW; modulation, 10 G. Simulation parameters: $S = 2$, $g = 2.0$, $D = -2$ cm^{-1}, $E/D = 0.13(3)$, $A = 160$ MHz.

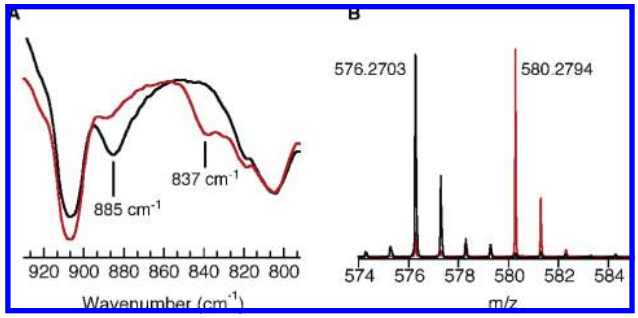

Figure 3. FTIR (A) and negative-mode ESI-MS (B) spectra of **2** after exposure to $^{16}O_2$ (black) and $^{18}O_2$ (red) collected from DMA solutions at room temperature.

under a $^{16}O_2$ atmosphere (Figure 3A). The ^{18}O-isotopomer can be prepared from $^{18}O_2$, causing a shift in the peak to 837 cm^{-1}. The observed vibrational change between the two isotopomers is as expected based on a harmonic O−O oscillator ($\nu(^{16}O_2)/\nu(^{18}O_2) = 1.06$; calcd = 1.07).[14] These vibrational values are in the range normally observed for other metal-based peroxo systems. For instance, the η^2-peroxoMn^{III}(Tp)[15] complexes of Kitajima, formed using H_2O_2, have FTIR-active peaks at 892 cm^{-1} that were assigned to $\nu(O_2)$.[6a] The electrospray ionization mass spectrum (ESI-MS) of **2** prepared with $^{16}O_2$ exhibits a strong ion with a mass-to-charge ratio (m/z) of 576.2703 (Figure 3B), a shift of 33 mass units from the peak associated with **1** (Figure S3). The mass and calculated isotopic distribution corresponds to the addition of a hydroperoxo ligand to **1** (calcd, 576.2706; Figure S4A). Furthermore, when **2** was prepared from $^{18}O_2$, the molecular ion peak shifts by 4 mass units (Figure 3B) to a m/z of 580.2794 (calcd, 580.2792; Figure S4B).

Preliminary reactivity studies indicate that **2** leads to the oxidative deformylation of aldehydes. For instance, treating **2** with cyclohexanecarboxaldehyde afforded cyclohexanone as the only GC−MS detectable product in an unoptimized yield of 40% (eq 1). Note that deformylation reactions are known for iron(III)[16] and manganese(III)[6b] peroxo complexes.

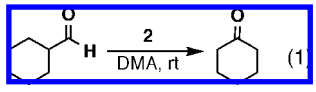

(1)

The spectroscopic, mass spectrometry, and reactivity results are consistent with **2** being a monomeric peroxomanganese(III) complex. A possible mechanism for its formation would involve a superoxomanganese(III) intermediate that reacts with solvent or external substrates, such as DPH, via a H-atom abstraction process to initially produce a η^1-hydroperoxoMn(III) complex (Figure 1, **2a**). The reduction and protonation of the superoxo ligand mirrors steps proposed during turnover in cytochrome P450. The tautomeric η^2-peroxomanganese(III) species (Figure 1, **2b**) could be formed from **2a** by intramolecular proton transfer from the hydroperoxo to the carboxamido component of the tripodal ligand. In this pathway, the pivaloylamide moiety is re-formed to provide an additional H-bond donor within the cavity. At present, we cannot distinguish between these two structural possibilities. Nevertheless, our findings establish that a mononuclear peroxoMn(III) can be produced from O_2 at room temperature.

Acknowledgment is made to the NIH (GM050781 to A.S.B.; GM77387 to M.P.H.) for financial support.

Supporting Information Available: Experimental details for all chemical reactions and figures for all spectra. This material is available free of charge via the Internet at http://pubs.acs.org.

References

(1) Borovik, A. S.; Zart, M. K.; Zinn, P. J. In *Activation of Small Molecules: Organometallic and Bioinorganic Perspectives*, Tolman, W. B., Ed.; Wiley-VCH: Weinheim, Germany, 2006; pp 187−234, and references therein.
(2) (a) *Cytochrome P450: Structure, Mechanism, and Biochemistry*, 3rd ed.; Ortiz de Montellano, P. R., Ed.; Kluwer Academic/Plenum Publishers: New York, 2005. (b) *Comprehensive Coordination Chemistry II*; Que, L., Jr., Tolman, W. B., Eds.; Elsevier: Oxford, 2004; Vol. 8. (c) Decker, A.; Chow, M. S.; Kemsley, J. N.; Lehnert, N.; Solomon, E. I. *J. Am. Chem. Soc.* **2006**, *128*, 4719–4733. (d) Groves, J. T.; Han, Y.-Z. In *Cytochrome P-450. Structure, Mechanism and Biochemistry*; Ortiz de Montellano R. R., Ed.; Plenum Press: New York, 1995; pp 3−48.
(3) Bossek, U.; Weyhermüller, T.; Wieghardt, K.; Nuber, B.; Weiss, J. *J. Am. Chem. Soc.* **1990**, *112*, 6387–6388.
(4) Dioxygen adducts of manganese porphyrins have been observed at low temperatures: (a) Weschler, C. J.; Hoffman, B. M.; Basolo, F. *J. Am. Chem. Soc.* **1975**, *97*, 5278–5280. (b) Hoffman, B. M.; Weschler, C. J.; Basolo, F. *J. Am. Chem. Soc.* **1976**, *98*, 5473–5482.
(5) (a) Shirazi, A.; Goff, H. M. *J. Am. Chem. Soc.* **1982**, *104*, 6318–6322. (b) Groves, J. T.; Watanabe, Y.; McMurry, T. J. *J. Am. Chem. Soc.* **1983**, *105*, 4489–4490. (c) VanAtta, R. B.; Strouse, C. E.; Hanson, L. K.; Valentine, J. S. *J. Am. Chem. Soc.* **1987**, *109*, 1425–1434. (d) Groni, S.; Blain, G.; Guillot, R.; Policar, C.; Anxolabehere-Mallart, E. *Inorg. Chem.* **2007**, *46*, 1951–1953.
(6) (a) Kitajima, N.; Komatsuzaki, H.; Hikichi, S.; Osawa, M.; Moro-oka, Y. *J. Am. Chem. Soc.* **1994**, *116*, 11596–11597. (b) Seo, M. S.; Kim, J. Y.; Annaraj, J.; Kim, Y.; Lee, Y.-M.; Kim, S.-J.; Kim, J.; Nam, W. *Angew. Chem., Int. Ed.* **2007**, *46*, 377–380.
(7) Borovik, A. S. *Acc. Chem. Res.* **2005**, *38*, 54–61, and references therein.
(8) Parsell, T. H.; Behan, R. K.; Hendrich, M. P.; Green, M. T.; Borovik, A. S. *J. Am. Chem. Soc.* **2006**, *128*, 8728–8729.
(9) (a) Wada, A.; Harata, M.; Hasegawa, K.; Jitsukawa, K.; Masuda, H.; Mukai, M.; Kitagawa, T.; Einaga, H. *Angew. Chem., Int. Ed.* **1998**, *37*, 798–799. (b) Mareque Rivas, J. C.; Salvagni, E.; Parsons, S. *Dalton Trans.* **2004**, 4185–4192. (c) Rudzka, K.; Arif, A. M.; Berreau, L. M. *J. Am. Chem. Soc.* **2007**, *128*, 17018–17023.
(10) Full experimental details are found in Supporting Information.
(11) Yields are obtained from EPR simulations using SpinCount developed by one of the authors (M.P.H.).
(12) The extinction coefficient for this peak is less than 300 M^{-1}cm^{-1}.
(13) (a) Campbell, K. A.; Yikilmaz, E.; Grant, C. V.; Gregor, W.; Miller, A.-F.; Britt, R. D. *J. Am. Chem. Soc.* **1999**, *121*, 4714–4715. (b) Campbell, K. A.; Force, D. A.; Nixon, P. J.; Dole, F.; Diner, B. A.; Britt, R. D. *J. Am. Chem. Soc.* **2000**, *122*, 3754–3761. (c) Campbell, K. A.; Lashley, M. R.; Wyatt, J. K.; Nantz, M. H.; Britt, R. D. *J. Am. Chem. Soc.* **2001**, *123*, 5710–5719. (d) Krzystek, J.; Telser, J.; Hoffman, B. M.; Brunel, L.-C.; Licoccia, S. *J. Am. Chem. Soc.* **2001**, *123*, 7890–7897.
(14) The difference of 48 cm^{-1} between the $\nu(O_2)$ of the two isotopomers is similar to those reported for Fe^{III}−OOH and Fe^{III}−OO complexes: Roelfes, G.; Vrajmasu, V.; Chen, K.; Ho, R. Y. N.; Rohed, J.-U.; Zondervan, C.; Crois, R. M.; Schudde, E. P.; Lutz, M.; Spek, A. L.; Hage, R.; Feringa, B. L.; Münck, E.; Que, L., Jr *Inorg. Chem.* **2003**, *42*, 2639–2653.
(15) Tp, hydrotris(3,5-*i*Pr-pyrazolyl)borate.
(16) (a) Vaz, A. D. N.; Roberts, E. S.; Coon, M. J. *J. Am. Chem. Soc.* **1991**, *113*, 5887–5889. (b) Selke, M.; Sisemore, M. F.; Valentine, J. S. *J. Am. Chem. Soc.* **1996**, *118*, 2008–2012. (c) Wertz, D. L.; Sisemore, M. F.; Selke, M.; Driscoll, J.; Valentine, J. S. *J. Am. Chem. Soc.* **1998**, *120*, 5331–5332. (d) Goto, Y.; Wada, S.; Morishima, I.; Wantanabe, Y. *J. Inorg. Biochem.* **1998**, *69*, 241–247.

JA802775E